On the stability of planar fluid interfaces under van der Waals surface forces

2003 J. Phys. A: Math. Gen. 36 8829

(http://iopscience.iop.org/0305-4470/36/33/308)

INSTITUTE OF PHYSICS PUBLISHING JOURNAL OF PHYSICS A: MATHEMATICAL AND GENERAL

J. Phys. A: Math. Gen. **36** (2003) 8829–8850 PII: S0305-4470(03)63106-9

On the stability of planar fluid interfaces under van der Waals surface forces

Stanley J Miklavcic

Department of Science and Technology, University of Linköping, S-601 74, Norrköping, Sweden

Received 8 May 2003
Published 5 August 2003
Online at stacks.iop.org/JPhysA/36/8829

Abstract

This paper concerns an analysis of the stability of infinite planar interfaces between two immiscible fluids. The interface is subjected to a two-dimensional stress arising from the van der Waals interaction with a solid, infinite plate of finite thickness, positioned edge-on to the interface. The physical problem models the setup of a Wilhelmy plate experiment just prior to plate immersion through a fluid interface and three-phase contact line formation. The van der Waals surface force is attractive, causing the fluid interface to deform. We investigate the stability of the fluid interface and establish an analytical condition which is sufficient to ensure a stable interface as well as a condition for which the interface will not be stable to arbitrary disturbances. Both conditions focus on a sole, key function of the equilibrium profile, the latter a solution of the Euler–Lagrange equation for the system.

PACS numbers: 47.20.−k, 82.70.Dd

1. Introduction

A technique commonly used in the field of surface chemistry to investigate interfacial tension is the Wilhelmy plate method [1, 2]. In this technique a rectangular plate of material, normally platinum, is immersed edge-on into a large-area trough of water exposed to air at atmospheric pressure and room temperature. The determination of the interfacial tension is accomplished by measuring the (net) amount of force required to support the plate against the force due to surface tension. Since the dispersal of molecules having an affinity for the air–water interface has an effect on the interfacial tension, properties of the surface and its constituent molecules can be deduced by a comparison of the measured tension as a function of mean molecular area [1]. Applications of this technique extend to dispersed surfactants or lipids [2, 3], proteins [4–6] , polymers [2] and other surface active molecules, including mixed systems, i.e. those involving two or more components. The technique is naturally not limited to the air–water interface, though this is the most common. It has, for example, also been used in studies of interfaces between other immiscible fluids, such as oil and water.

0305-4470/03/338829+22$30.00

A considerable amount of work on the theoretical modelling of the mechanics of the Wilhelmy plate technique [1] as well as modelling of the phase behaviour of the two-dimensional distribution of the surface active molecules exists [7]. However, in this paper we divert attention from the surface tension measurement per se, albeit the most important feature of the technique, to the more esoteric, pre-immersion configuration in which the plate is in close vicinity to the interface. When in close proximity, but prior to three-phase contact, a surface force of van der Waals type arises. The strength of this force is measured by a Hamaker constant [8], a function of the bulk dielectric properties of the three media. This van der Waals surface force, while short ranged, extends over a finite area of the fluid–fluid surface and causes it to deform from its original flat shape. It is this deformation which is investigated in this paper. In particular, we are interested in the following phenomena described in the context of the air–water interface.

As the plate approaches the interface the water surface increases its deformation as a result of the increasing attraction. At some finite height above the base water level or finite proximity to the plate, the deformed water surface can no longer maintain its continuous and smooth elongated shape. Indeed, at some finite separation, the water interface jumps up and captures the plate, establishing three-phase contact. Determining this point of instability and what it depends on is our essential goal. This paper contributes to this goal by providing some mathematical foundations for understanding the stability and instability states. The analysis and conclusions are not specific to any particular choice of two immiscible fluids. For this reason the work is presented in a more general context; the interface between the two arbitrary immiscible fluids we refer to as the fluid interface, for brevity.

It should be emphasized that it is the *equilibrium* stability of a free interface under external stress that is studied in this paper. The techniques and results are to be distinguished from studies of the dynamic stability of interfaces either due to hydrodynamic stresses or combinations of hydrodynamic and other external stresses [9–12]. Equilibrium stability studies following various theoretical approaches have been carried out on systems of interacting thin films supported on solid substrates [13, 14] in order to quantify capillary condensation. These systems, however, are too distinct for those results to be relevant to the present problem. On the other hand, an equilibrium analysis of an axisymmetric (as opposed to mirror-symmetric) system related to that studied here has been considered in [15], although without an explicit treatment of stability. While mechanical limits of stability in terms of equation solvability limits were discovered and discussed (a feature we discuss in an extensive study [16, 17]), such mathematical limits, representing absolute bounds, are to be distinguished from physical stability limits. The latter may ensure that the former are never attained in practice.

To assist the reader in his or her examination of the material in this paper we summarize the most important features and results.

We begin in section 2 by setting up a physical model for the two-dimensional plate–fluid interface system, illustrated in figure 1. Contributions to the total free energy of the system are written in terms of an arbitrary fluid interface profile denoted as $\overline{z}(x)$; x being the sole independent coordinate variable appearing in this two-dimensional problem. These contributions are collected in the total energy which is then expanded about the optimum profile, $z(x)$, defined as that profile which zeros the first-order term in this expansion [18]. This is the essence of the variational approach [19, 20]; the optimum profile is required to be the solution of the Euler–Lagrange equation corresponding to this vanishing first-order term. We give examples of solutions to this Euler–Lagrange equation for some parameter values.

The focus thereafter is on the status of the second-order term in the energy expansion which governs whether the optimum profile is a local minimizer of the free energy, a local

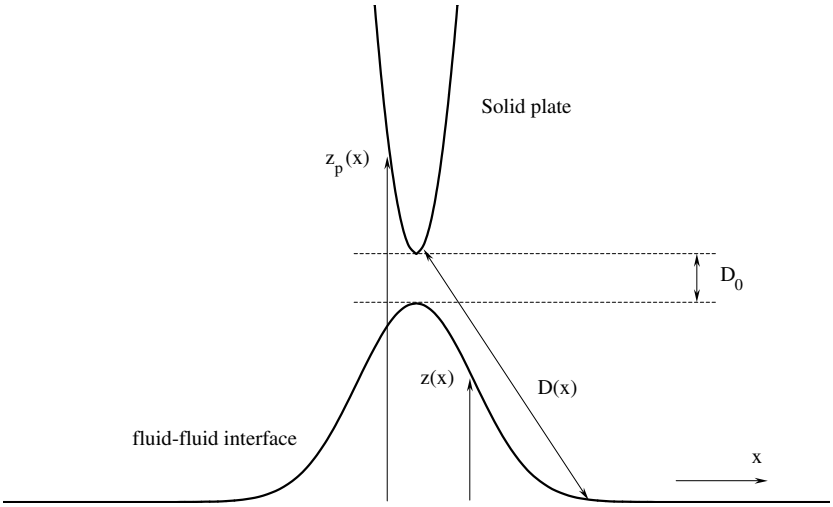

Figure 1. Schematic diagram depicting the cross-sectional geometry of the plate–fluid–fluid system. The solid plate shown has the form of a parabolic cylinder with cross-section $z_p(x) = z_{p0} + \lambda x_p^2$, while the fluid interface is described by the function, $z(x)$. The distance $D(x, z)$ is defined in the direction of the solid surface vector normal.

maximizer or a profile associated with a local saddle point of the free energy surface. These mathematical states correspond to the physical states of stability, instability and marginal stability, respectively. Consequently, in section 3 we address this stability question. The most important feature of section 3 is the result of a reformulation of the second-order free energy term which introduces a single function, $\Phi = \Phi(x)$, defined in (22). This sole function, Φ, is explicitly dependent on the optimal profile, $z(x)$. The dependence is intricate indicating that Φ must generally be determined numerically. In this section we give examples of the function's general appearance as well as its dependence on physical parameters.

In section 4 we present the key results of this paper: sufficient conditions governing the stability state of the optimum profile assuming only that Φ conforms to certain expectations. Using quite disparate approaches we establish (a) that if Φ, however it may appear in detail, satisfies the condition, $l_G^2\Phi(x) \geqslant K - (K+4)\exp\left(-x^2/l_G^2\right)$, for some given interaction-independent positive constants, K and l_G, then the profile $z(x)$ will be stable to all (small) perturbations, and (b) if $l_G^2\Phi(x) \leqslant K - (K + f(K))\exp\left(-x^2/l_G^2\right)$, where $f(K)$ is an established positive function of K, then the profile $z(x)$ cannot be stable to arbitrary perturbations. We discuss and demonstrate the utility of these sufficient conditions using the examples of section 3. Important details of the proofs of these sufficient conditions using rigorous arguments are given in the appendix.

2. The equilibrium shape of the air–water interface

When the interface experiences the van der Waals stress the attraction that is manifested between the plate and fluid interface causes the interface to deform, leading to a bulge in the fluid surface beneath the plate. Associated with this deformation is a change in free energy. Part of this change is represented by a gravitational potential term coming from the mass of underlying fluid raised above the $z = 0$ reference plane. A further contribution is a surface energy term arising from the increased surface area of fluid–fluid contact. Finally, there is the

energy of interaction between the plate and fluid surface represented as a surface integral of the surface energy density, σ. When deformed the free energy of the fluid interface changes by

$$F = \gamma A_\Lambda + G \int\int\int_{\Delta V_\Lambda} z \, \mathrm{d}V + \int\int_\Lambda \sigma \, \mathrm{d}S. \tag{1}$$

In (1) $G = g\Delta\rho$, with fluid density difference $\Delta\rho$ and acceleration due to gravity, g; the intrinsic interfacial tension is γ. The terms in (1) are, respectively, the surface energy associated with the surface area change, the gravitational potential energy term and finally the interaction term. Λ denotes the deformed interface.

We shall implicitly suppose that the stress acting over the surface possesses everywhere continuous partial derivatives up to order k, with fixed $k \geqslant 2$. That is, $\sigma \in C^k(\mathbb{R}^2)$, for some $k \geqslant 2$.

The free energy change (1) defines a functional over a space of functions, Ω_x, which represents the set of all possible profiles of the fluid interface. As the plate positioned edge-on over the infinite surface is assumed infinitely long (e.g., a regular parabolic cylinder as depicted in figure 1), the problem becomes two-dimensional. Consequently, the free energy reduces to a one-dimensional integral

$$F = \gamma \int_{-\infty}^{\infty} W(\overline{z}_x(x)) \, \mathrm{d}x + \frac{1}{2} G \int_{-\infty}^{\infty} \overline{z}(x)^2 \, \mathrm{d}x + \int_{-\infty}^{\infty} W(\overline{z}_x(x)) \sigma(x, \overline{z}(x)) \, \mathrm{d}x$$

where $W(p) = (1 + p^2)^{1/2}$. The functional, F, is clearly a free energy per unit length, expressed as an (improper) integral of the multivariable function of $(x, \overline{z}, p)$

$$f(x, \overline{z}, p) = W(p)h(x, \overline{z}) + \tfrac{1}{2} G \overline{z}^2 \tag{2}$$

where $h := \gamma + \sigma$. W is a C^∞-function; since σ (or h) is a C^k-function for $k \geqslant 2$, so too is f. Both the equilibrium shape of the fluid interface and its state of stability are determined through analyses of the first and second variations of the energy functional

$$F[\overline{z}] = \int_{-\infty}^{\infty} f(x, \overline{z}(x), \overline{z}_x(x)) \, \mathrm{d}x \tag{3}$$

with respect to functions $\overline{z}$ belonging to an appropriate class, Ω_x. In fact, from the physical considerations of the problem we define Ω_x to be the space of even, integrable functions, η, that possess continuous second-order derivatives each of which is square integrable,

$$\int_{-\infty}^{\infty} |\eta^{(k)}|^2 \, \mathrm{d}x < \infty \qquad k = 0, 1, 2.$$

That is, we define the set

$$\Omega_x = \{\eta : \eta^{(k)} \in C(\mathbb{R}) \cap L_2(\mathbb{R}), k = 0, 1, 2; \eta(x) = \eta(-x)\}. \tag{4}$$

Here, $L_2(\mathbb{R})$ is the space of square integrable functions [24].

Because of smoothness these functions necessarily satisfy the condition $\eta_x(0) = 0$. Herewith, we shall suppose the existence of a function, $z \in \Omega_x$, hereafter referred to as the equilibrium profile, that gives an extreme value to the functional F. Furthermore, we shall assume that it is unique.

Consider an arbitrary $\overline{z} \in \Omega_x$. A suitable element, $\eta \in \Omega_x$, and a real number, ϵ, can be found to satisfy the equality, $\overline{z}(x) = z(x) + \epsilon\eta(x)$. The parameter, ϵ, will hereafter play the role of an expansion parameter. Note that, since f is a C^k-function, F can be considered a C^k-function of the parameter, ϵ, for $k \geqslant 2$. That is, for any fixed $\eta \in \Omega_x$

$$g(\epsilon) := F[z + \epsilon\eta]$$

is at least a C^2-function of ϵ. Presuming that all requirements are met for a second-order Taylor polynomial approximation to $g(\epsilon)$, we can write

$$g(\epsilon) = g(0) + \epsilon g'(0) + \frac{\epsilon^2}{2} g''(0) + O(\epsilon^3). \tag{5}$$

The first term of (5) corresponds to the functional, F, evaluated at the equilibrium profile, z. According to the fundamental theorem of variational calculus [20], the vanishing of the second term of (5) leads to the Euler–Lagrange equation for z. Invoking the first partial derivatives of $f(x, z, p)$ with respect to z and p,

$$\begin{cases} f_z = Gz + h_z(x, z)W(p) \\ f_p = \frac{h(x,z)p}{W(p)} \end{cases} \tag{6}$$

we obtain the Euler–Lagrange equation satisfied by the equilibrium solution, z,

$$\left(\frac{h(x, z)z_x}{W(z_x)} \right)_x = Gz + h_z(x, z)W(z_x). \tag{7}$$

2.1. Numerical examples of the equilibrium profile

The relevant interaction between the fluid interface and the 2D solid across an immiscible fluid gap is the van der Waals interaction [8]. To compute this exactly is a nontrivial task, even if the fluid interface shape was fixed. Instead, we shall use the simplifying assumption that the van der Waals surface energy density, σ, is that obtained from the surface stress, π. In turn π is based on the van der Waals pressure acting between two infinite parallel planar surfaces separated by a distance, D [8]

$$\pi(D) = -\frac{C_H}{D^3}.$$

C_H is the Hamaker constant, a parameter dependent on the dielectric properties of the three material media. From this pressure one obtains the surface free energy density by integration

$$\sigma(D) = -\int_{\infty}^{D} \pi(\tau)\, \mathrm{d}\tau = -\frac{C_H}{2D^2}. \tag{8}$$

Although, we implement (8) in numerical examples as the van der Waals interaction, it should be known that this is but an approximation to the true van der Waals interaction. However, the Derjaguin approximation [8] justifies using this expression in cases of low curvature objects. The distance function, $D = D(x, z)$, appearing in this expression depends on the independent variables x and z. In the numerical work the solid is a parabolic cylinder, positioned edge-on adjacent to the fluid interface. The cylinder's cross-sectional profile obeys the equation, $z_p(x) = z_{p0} + \lambda x_p^2$, (see figure 1). (x_p, z_p) are the 2D coordinates of an arbitrary point on the cross-section. z_{p0} is the minimum height of the solid at the apex above the undeformed fluid surface and $\lambda > 0$ is a curvature parameter we refer to as the splay constant. The distance function is defined as the distance from a point, (x_p, z_p), on the surface of the plate to the unique point, $(x, z(x))$, on the fluid interface, in the direction of the outward normal to the plate. That is,

$$D(x, z) = \sqrt{(x - x_p)^2 + (z(x) - z_p)^2} \tag{9}$$

where the points $(x, z(x))$ and (x_p, z_p) are related by the vector equation

$$\nabla_p \left(z_0 + \lambda x_p^2 - z_p \right) = \alpha(x - x_p, z(x) - z_p).$$

$\nabla_p = \left(\frac{\partial}{\partial x_p}, \frac{\partial}{\partial z_p}\right)$ and α is a proportionality constant providing equality between the vector joining the two points in question and the plate's surface vector normal. Upon eliminating α we obtain an equation for x_p in terms of x:

$$(x - x_p) = 2\lambda x_p \left(z_0 + \lambda x_p^2 - z(x)\right) \quad \Longleftrightarrow \quad 2\lambda^2 x_p^3 + x_p(1 + 2\lambda(z_0 - z(x))) - x = 0.$$

The physically relevant root of this cubic equation establishes $x_p = x_p(x)$. In fact, the nature of the cubic indicates that there is only one physically viable root,

$$x_p(x) = R - \frac{1 + 2\lambda(z_0 - z(x))}{6\lambda^2 R} \tag{10}$$

where

$$R = \left[\frac{x}{4\lambda^2} + \sqrt{\frac{x^2}{16\lambda^4} + \frac{(1 + 2\lambda(z_0 - z(x)))^3}{216\lambda^6}}\right]^{1/3}. \tag{11}$$

The two remaining roots are complex (conjugates). Thus, the distance function, $D(x, z(x))$, depends on x either explicitly or implicitly via the optimal profile $z(x)$.

In the far field, i.e. far from the vicinity of the plate, the localized van der Waals stress ceases to have an explicit effect. Futhermore, the condition $|z_x| \ll 1$ is satisfied. Equation (7) then simplifies to the linear equation

$$\gamma z_{xx} = Gz$$

with exponential solution

$$z(x) = C\,\mathrm{e}^{-|x|/l_G} \qquad |x| \gg 1 \tag{12}$$

where $l_G = \sqrt{\gamma/G}$ is the characteristic decay length, traditionally denoted by the capillary length. Naturally, a positive constant, C, is consistent with an attractive interaction between the plate and interface. Its value is chosen to match this far-field solution with the near-field solution.

Numerical solution of (7) with (8) and (9) for the near-field is achieved using a fourth-order Runge–Kutta algorithm, with boundary conditions applied on the ends of a finite interval $[0, x_\infty]$ for some conveniently selected extreme x-value, x_∞:

$$\begin{cases} z_x(0) = 0 \\ z\,(x_\infty) = C\,\mathrm{e}^{-x_\infty/l_G}. \end{cases} \tag{13}$$

A numerical root-finding procedure was applied to the remaining end condition

$$z_x(x_\infty) = -C\,\mathrm{e}^{-x_\infty/l_G}/l_G \quad \Longrightarrow \quad z_x(x_\infty) + z(x_\infty)/l_G = 0 \tag{14}$$

in order to determine the initial profile value, $z(0) = z_0$. The value of the constant coefficient, C, is then determined. Further details of the calculation method can be found in [17].

In figure 2 we show examples of fluid interface profiles for a selected Hamaker constant, C_H, and splay parameter, λ, for various plate heights, z_{p0}. Results for other parameter choices are similar in character to these. On this scale the corresponding far-field solutions, (12), projected all the way to $x = 0$, are all but indistinguishable from the exact numerical solutions to (7) shown. In the example calculations a matching of (13) and (14) was performed assuming $x_\infty = 0.1$ m in order to obtain the full solution. For the selected value, $\lambda = 0.1$, both the plate and the responding fluid profile have small curvature. Consequently, the conditions under which (8) can be implemented are satisfied.

The most significant aspect of these results is the disparity in the two orthogonal length scales. The vertical extent of deformation is only of the order of several hundreds of nanometres, while the lateral extent of deformation is of the order of a significant fraction of

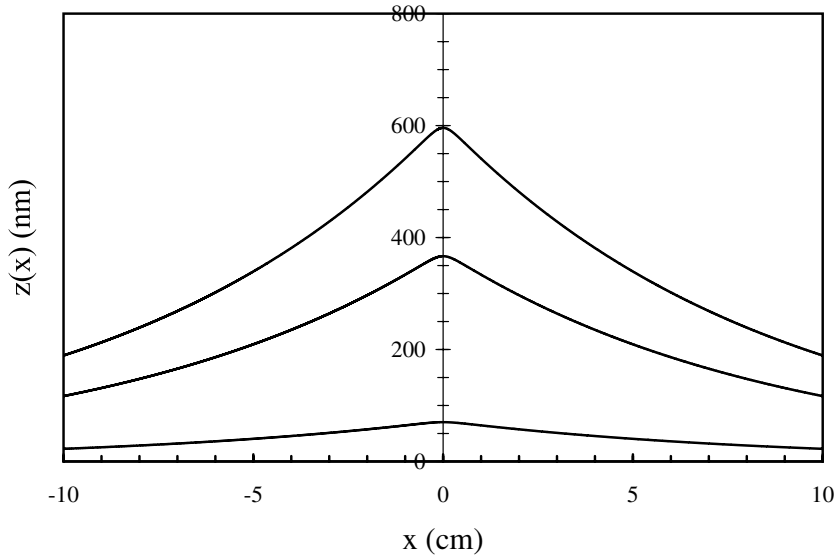

Figure 2. Equilibrium fluid interface profiles. Physical parameters adopted are $\Delta\rho = 1$ kg m^{-3}, $\gamma = 72.8$ mN m^{-1}, and a Hamaker constant of $C_H = 10^{-21}$ J. The curves result from the interaction with a parabolic plate of height (top to bottom): $z_{p0} = 2270, 2400, 4000$ nm. The plate's splay parameter, $\lambda = 0.1$ m^{-1}.

a metre. The vertical deformation is characterized more by a length scale determined from a complex combination of the length scale $l_H = \sqrt{C_H/\gamma}$ (0.12 nm) and the geometric lengths λ and z_{p0}, than by the capillary length scale l_G, here equal to 8.63 cm, which is what governs the lateral extent. In such cases the lateral extent of the ensuing deformation may not be apparent to the naked eye. This feature has also been found in related studies of an axisymmetric system [17]. In that paper and in [16] we also point out that a solution to an equation such as (7) is not always possible. This indicates that there exist mathematical limits to how close one can position the plate to the fluid interface. What we consider in the remaining paper are the *physical* limits to the closest approach distance. These limits, founded on energy arguments, show that even when a mathematical solution exists this may not be stable to even small disturbances and therefore the profile is not likely to eventuate in practice. Again, we suppose that an equilibrium profile, found by solving (7), does exist and is unique.

3. The stability of the air–water interface under stress

If the equilibrium profile is a minimizing profile then it must necessarily satisfy (7). However, not every solution of (7) need constitute a minimum of the functional (3). That is, not every solution, say ξ, need satisfy the inequality

$$F[\xi] = \int_{-\infty}^{\infty} f(x, \xi(x), \xi_x(x))\,\mathrm{d}x \leqslant F[\overline{z}] \tag{15}$$

for all other $\overline{z} \in \Omega_x$ with equality occurring only for $\overline{z} = \xi$. To establish whether a solution z is a minimizing profile one must look to the next term in the parameter expansion (5).

For sufficiently small ϵ the sign of the third term, called the second variation of the functional, F, adequately determines the minimum or maximum or saddle point character

of z. In physical terms, the *sign* of the second variation determines whether the equilibrium profile is *stable* or *unstable* to small perturbations. The second variation, expressed as [19]

$$\delta^2 F = \frac{\epsilon^2}{2}\left(\left.\frac{\partial^2 F}{\partial \epsilon^2}\right|_{\epsilon=0}\right) = \frac{\epsilon^2}{2} g''(0)$$

involves the derivative, $\partial^2 f/\partial \epsilon^2$, evaluated at $\epsilon = 0$, i.e. at the equilibrium solution, $z(x)$:

$$\left.\left(\frac{\partial^2 f}{\partial \epsilon^2}\right)\right|_{\epsilon=0} = f_{zz}\eta^2(x) + 2 f_{zz_x}\eta(x)\eta_x(x) + f_{z_x z_x}\eta_x^2(x).$$

By means of a partial integration, the second variation of F can thus be written as [18, 22]

$$\delta^2 F = \frac{\epsilon^2}{2}\int_{-\infty}^{\infty}\left[f_{z_x z_x}\eta_x^2(x) + \left(f_{zz} - \left(f_{zz_x}\right)_x\right)\eta^2(x)\right]\mathrm{d}x. \tag{16}$$

The second partial derivatives of $f(x, z, p)$, treated as a function of independent variables, x, z and $p(=z_x)$ occurring in this integral are, respectively,

$$\begin{cases} f_{pp} = \frac{h(x,z)}{(1+p^2)^{3/2}} \\ f_{zz} = G + h_{zz}(x, z)(1 + p^2)^{1/2} \\ f_{zp} = \frac{p h_z(x,z)}{(1+p^2)^{1/2}}. \end{cases} \tag{17}$$

Note that $f_{zp} = 0$, $f_{zz} = G$ and $f_{z_x z_x} > 0$ in the case $h \equiv \gamma$, i.e. in the absence of any externally imposed surface stress.

3.1. Reformulation of the second variation

An analysis of the stability of the equilibrium profile is hampered by the presence of the two coefficient functions multiplying the terms η^2 and η_x^2 in the integrand of (16). Both of these contributions depend on the profile, $z(x)$; they vary in magnitude and can, legitimately, be either positive or negative. However, the difficulty diminishes if we rewrite the second variation (16) so as to eliminate one of the coefficients. For this reformulation (presented below) to be valid, however, we must insist that the function f_{pp} be strictly positive in its domain of definition. From (17) it is clear that this will hold provided $h(x, z) \equiv \gamma + \sigma(x, z)$ is strictly positive for all points (x, z). As the bulk of this work deals with van der Waals interactions for the three different media, solid–fluid–fluid, in which the intervening medium has dielectric properties intermediate of the three, one anticipates [8] that $\sigma < 0$. The analysis below is thus limited to interaction strengths such that $\max|\sigma| < \gamma$. By (8) this restraint gives an upper bound on the allowed Hamaker constant for a fixed separation. Alternatively and more appropriately, for a given Hamaker constant it gives a lower bound on the minimum possible separation between the plate and the fluid interface, namely,

$$D_{\min} > \left(\frac{C_H}{2\gamma}\right)^{1/2}. \tag{18}$$

For example, for the air–water interface and water–air–metal system, (18) gives a lower bound for the minimum allowed separation of the order of 1 nm.

Recall (16) (modulo the unimportant prefactor of $\epsilon^2/2$):

$$\delta^2 F = \int_{-\infty}^{\infty}\left[f_{z_x z_x}\eta_x^2(x) + \left(f_{zz} - \left(f_{zz_x}\right)_x\right)\eta^2(x)\right]\mathrm{d}x. \tag{19}$$

If (18) (or more generally, $f_{pp} > 0$) holds one can invoke the transformation $v = (f_{pp})^{1/2}\eta$ where $\eta \in \Omega_x$, to find that

$$v_x = [(f_{pp})^{1/2}]_x \eta + (f_{pp})^{1/2}\eta_x. \tag{20}$$

Note that $v \to 0$ as $|x| \to \infty$. Also, as $h_x(0, z(0)) = 0$ from the condition of symmetry, we deduce from (17), that $(f_{pp})_x = 0$ at $x = 0$. Hence, $v_x(0) = 0$ if $\eta \in \Omega_x$. Therefore, v itself belongs to the space Ω_x. From (20) we find that

$$\begin{aligned} f_{pp}\eta_x^2(x) &= [v_x - [(f_{pp})^{1/2}]_x \eta]^2 \\ &= v_x^2 + \left[\frac{1}{2}\left(\frac{(f_{pp})_x}{f_{pp}}\right)_x + \frac{[(f_{pp})_x]^2}{4f_{pp}^2}\right] v^2 - \frac{1}{2}\left[\frac{(f_{pp})_x v^2}{f_{pp}}\right]_x . \end{aligned}$$

Consequently, in (19) make the substitution

$$f_{z_x z_x}\eta_x^2(x) + \left(f_{zz} - \left(f_{zz_x}\right)_x\right)\eta^2(x) = v_x^2 + \Phi(x)v^2 - \frac{1}{2}\left[\frac{(f_{pp})_x v^2}{f_{pp}}\right]_x \tag{21}$$

where the function

$$\begin{aligned} \Phi(x) &= \frac{1}{2}\left(\frac{(f_{pp})_x}{f_{pp}}\right)_x + \frac{[(f_{pp})_x]^2}{4f_{pp}^2} + \frac{\left(f_{zz} - \left(f_{zz_x}\right)_x\right)}{f_{pp}} \\ &= \frac{2[(f_{pp})_{xx} + 2(f_{zz} - (f_{zp})_x)]f_{pp} - [(f_{pp})_x]^2}{4f_{pp}^2} \end{aligned} \tag{22}$$

has been introduced. The various terms appearing in (22) are evaluated using the explicit expressions in (17) with $z(x)$ as the equilibrium profile. Inserting (21) into (19) and integrating the third term on the rhs we find

$$\delta^2 F = \int_{-\infty}^{\infty} \left[v_x^2 + \Phi(x)v^2\right] \mathrm{d}x - \frac{1}{2}\left[\frac{(f_{pp})_x v^2}{f_{pp}}\right]_{x=0}^{x\to\infty} .$$

The last term vanishes at the upper limit by the property $v(|x| \to \infty) \to 0$, inherited from the asymptotic behaviour of η. At the lower limit, the contribution vanishes again since $(f_{pp})_x = 0$, from the mirror symmetry of the physical problem.

In summary, the investigation of stability reduces to an analysis of the integral

$$I[v] := \delta^2 F = \int_{-\infty}^{\infty} \left[v_x^2 + \Phi(x)v^2\right] \mathrm{d}x \tag{23}$$

involving functions v over the space Ω_x.

The function, $\Phi(x)$, is the only function involving the equilibrium profile which needs to be considered. Although complicated in appearance it can be evaluated with knowledge of only $z(x)$ and $z_x(x)$. We demonstrate its general appearance and tendencies through examples in the next section. From symmetry we expect $\Phi(x)$ to be an even function of x (no physical change occurs with the transformation $x \to -x$). Consequently, as we only consider those functions v that belong to Ω_x we may replace the infinite integral by twice the integral over the semi-infinite interval $[0, \infty)$. Furthermore, as we are only interested in the sign of the second variation, we can and will ignore all positive constants that multiply this integral (e.g., the factor $2\epsilon^2/2$).

As a trivial precursor example consider the case of a free fluid–fluid interface, $z \equiv 0$. The surface stress, σ, is then zero, $h = f_{z_x z_x} = \gamma$, a constant, and the derivatives $f_{zp} = h_{zz} = 0$, while $f_{zz} = G > 0$, if the underlying fluid (say, water) is denser than that above (say, air). It is then easy to see that $\Phi(x) = G/\gamma$, a positive constant. From (23), the second variation will then be positive for all $v \in \Omega_x$, and the profile, $z = 0$, stable to all small perturbations. Naturally, the stability of this elementary case could equally well have been analysed directly using (16). The strength of the reformulation, however, becomes apparent in nontrivial cases involving a locally varying surface stress.

This simple example is nevertheless important to consider since the function Φ asymptotes precisely to this positive value in the limit $x \to \infty$ where the influence of the van der Waals stress is negligible and the deformed profile $z \to 0$:

$$\Phi(x) \to G/\gamma \qquad \text{as} \quad |x| \to \infty. \tag{24}$$

It now remains to establish how negative but finite the function $\Phi(x)$ can be in the neighbourhood of $x = 0$. Interest clearly focuses on how negative $\Phi(x)$ can be under typical circumstances in order for the functional $I[v]$ to remain positive for all v and therefore guarantee stability. We return to this question in the next section where in addition we also consider the contrary question of how negative Φ must be near $x = 0$ to ensure instability.

3.2. Numerical examination of the stability function Φ

The dependence of Φ on both the independent variable, x, and the profile, $z(x)$, is intricate, made worse by the complicated dependence (9) of the distance function, D, on these quantities via several others: $z_p(x) = z_{p0} + \lambda x_p^2$, (10) and (11). At the highest level of the calculation we have to consider the following terms in Φ:

$$\begin{cases} \frac{(f_{zz}-(f_{zz_x})_x)}{f_{pp}} = \frac{1}{h}[GW(z_x)^3 - h_z z_{xx} - (h_{zx}z_x + h_{zz})W(z_x)^2] \\ \frac{[(f_{pp})_x]^2}{4f_{pp}^2} = \frac{1}{4}\left[\frac{1}{h}(h_z z_x + h_z) - 3z_x z_{xx} W(z_x)^{-2}\right]^2 \end{cases}$$

and

$$\frac{1}{2}\left(\frac{(f_{pp})_x}{f_{pp}}\right)_x = \frac{1}{2}\left[\frac{6z_x^2 z_{xx}^2}{W(z_x)^4} - \frac{3\left(z_{xx}^2 + z_x z_{xxx}\right)}{W(z_x)^2} - \frac{(h_z z_x + h_z)^2}{h^2} + \frac{\left(h_{xx} + 2h_{zx}z_x + h_{zz}z_x^2 + h_z z_{xx}\right)}{h}\right].$$

The second and third derivatives of z can be evaluated with the help of the Euler–Lagrange equation (7). The various first and second partial derivatives of h require corresponding derivatives of the distance function, D. Partial derivatives of D with respect to x and z are both explicit and implicit through z_p and x_p. Further evaluation of these, however, is both tedious and unenlightening. Hence, we shall not present these explicit results here.

Figure 3 demonstrates typical Φ behaviour as a function of lateral extent. As mentioned earlier, physically one would expect that as either the Hamaker constant, C_H, is increased or the apex of the plate, z_{p0}, is lowered, or with any combination of these, the fluid interface would rise, eventually reaching some limit beyond which the lower fluid would preferentially wet the solid. This is translated mathematically into the expectation that Φ would become increasingly more negative thus giving cause for the functional, $I[v]$, to become negative for certain perturbations, v. At all times, however, Φ must satisfy the asymptotic condition (24). These expected trends in Φ are clearly confirmed in the numerical examples. Note that since $f_{z_x z_x}$ is strictly positive, Φ remains everywhere finite (in figure 3(*a*) the lowermost curve corresponding to the lowest height of the plate is bounded below by a finite negative value, $\Phi \approx -5110$, attained at $x = 0$). Some important details are worth explicitly pointing out. Since we consider the same fluid in both cases, the same asymptotic limit is approached, $G/\gamma = 134.34\ \text{m}^2$. Increasing either z_{p0} or the strength of the van der Waals stress serves to deepen the negative well about the origin; the x-range, however, does not change appreciably as this is mostly determined by the asymptotic behaviour of $z(x) \sim \exp(-|x|/l_G)$. Implementation of other

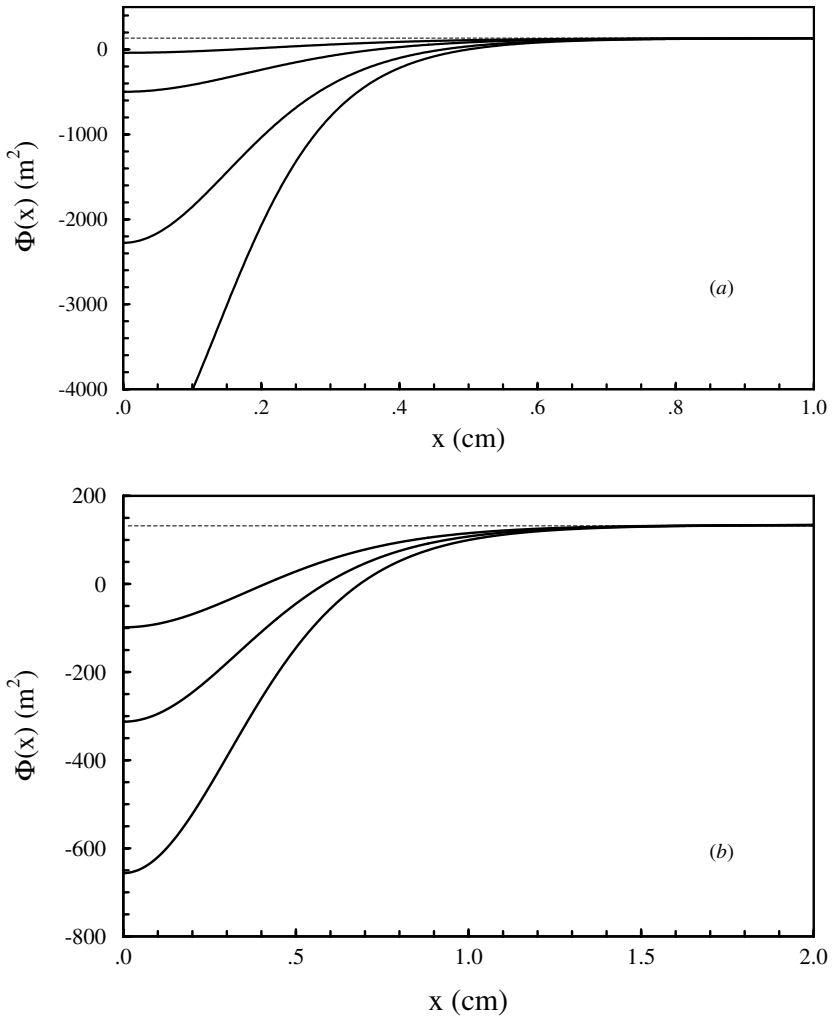

Figure 3. Plots of the stability function corresponding to the van der Waals interaction between a fluid interface and a parabolic plate of vertical cross-section, $z_p(x) = z_{p0} + \lambda x_p^2$, for a fixed splay parameter, $\lambda = 0.1\ \mathrm{m}^{-1}$. Other physical parameters are $\Delta\rho = 1\ \mathrm{kg\ m}^{-3}$, $\gamma = 72.8\ \mathrm{mN\ m}^{-1}$. In (*a*) the Hamaker constant, $C_H = 10^{-21}$ J, and the curves (bottom to top) refer to plate heights of $z_{p0} = 2270, 2400, 3000, 4000$ nm. In (*b*) $C_H = 10^{-19}$ J and the curves (bottom to top) refer to plate heights of $z_{p0} = 9500, 10\,500, 12\,000$ nm.

parameter values for G, C_H or λ does not change the impression already given by the examples in figure 3. What should be kept in mind, however, is that the parameter values themselves are not as important as their combinations determining the length scales, l_G and l_H. Features present in figure 3 do arise for other parameter values and will appear at similar locations when measured on a relative scale.

4. Sufficient conditions for stability and instability

In the previous section we demonstrated by rigorous argument and then by example that the derived stability function, Φ, of the equilibrium profile, $z = z(x)$, asymptotically approaches

a positive constant. Furthermore, numerical examples indicate that a constant (possibly negative) can be found such that Φ is bounded below. In fact, irrespective of the examples it is clear that provided $f_{z_x z_x} > 0$ for the Euler–Lagrange profile, $z = z(x)$, these same features will always appear for Φ. We summarize these facts in the following supposition. For some finite constants L and $U > 0$, suppose that Φ satisfies the conditions

$$\begin{cases} L < \Phi < U & \text{for all} \quad x \in \mathbb{R} \\ \Phi \to U & \text{as} \quad |x| \to \infty. \end{cases}$$

The remaining section addresses questions about the values of U and, in particular, L for which one can make definite statements about the stability of the equilibrium profile. Actually, as in [23] two complementary questions are addressed here. One concerns L values for which stability is guaranteed. The other concerns L values for which a profile is definitely unstable. In contrast to the methods used in [23], the proof of the following instability condition is based on a Ritz optimization, while the stability result is established using function inequality arguments. The proofs of these important and fundamental results are relegated to the appendix.

We note from section 2 the significance of the lateral length scale, $l_G = \sqrt{\gamma/G}$, associated with the solution to the Euler–Lagrange equation. Since Φ clearly depends explicitly on the profile, it too is governed by the same scaling. This motivates the introduction of the scaled variable $y = x/l_G$ into the second variation, (23), which thus becomes

$$I[v] = \int_{-\infty}^{\infty} \left[v_x^2(x) + \Phi(x)v^2(x)\right] \mathrm{d}x = \frac{1}{l_G} \int_{-\infty}^{\infty} \left[v_y^2(yl_G) + l_G^2 \Phi(yl_G)v^2(yl_G)\right] \mathrm{d}y$$
$$= \frac{1}{l_G} \int_{-\infty}^{\infty} \left[w_y^2 + \Psi(y)w^2\right] \mathrm{d}y. \tag{25}$$

The definition of $\Psi(y)$ as $l_G^2\Phi(yl_G)$ is fortuitously convenient. Asymptotically we find that

$$\Psi \to 1 \qquad \text{as} \quad |y| \to \infty \tag{26}$$

as a consequence of the asymptotic constant, $U = G/\gamma = 1/l_G^2$, from (24). Stability questions now focus on the normalized expression (modulo the irrelevant positive constant multiplier). The integral in (25) is the object of study of the appendix. There we establish that it will be positive definite if $\Psi(y) \geqslant K - E\,\mathrm{e}^{-y^2}$ for given $K > 0$ and if $E \leqslant K + 4$. On the other hand, it can be negative for some functions, w, if for given K, $\Psi(y) \leqslant K - E\,\mathrm{e}^{-y^2}$ when $E > 3[(29 - 3K)\sqrt{6} + \sqrt{3894 - 4500K + 2550K^2}]/32$. In the present particular application we have, from (25) and (26), that $K = 1$. We therefore have the following two corollaries (of lemmas 3 and 5) which state fundamental sufficient conditions for stability and instability, respectively, against infinitesimal disturbances. These are independent of any approximation involved in the choice of the surface stress function and require only that the interaction manifests itself in a locally varying surface energy density, leading to a surface energy contribution to the total free energy.

Condition 1 (Stability)**.** *Let $z \in \Omega_x$ be the solution of (7) for the equilibrium profile of the fluid interface subject to a local van der Waals stress. Furthermore, let $z(x)$ satisfy the constraint that $\Phi = \Phi(x, z(x))$ remain bounded as described in the beginning of this section, for all $x \in \mathbb{R}$. Then, there exists a positive constant E^* such that if*

$$\Phi(x) \geqslant \frac{1 - E\,\mathrm{e}^{-(x/l_G)^2}}{l_G^2} =: t(x) \qquad \forall x \in \mathbb{R} \tag{27}$$

for some $E \leqslant E^*$ then the equilibrium profile will be stable to arbitrary infinitesimal perturbations $v \in \Omega_x$. In fact, $E^* = 5$.

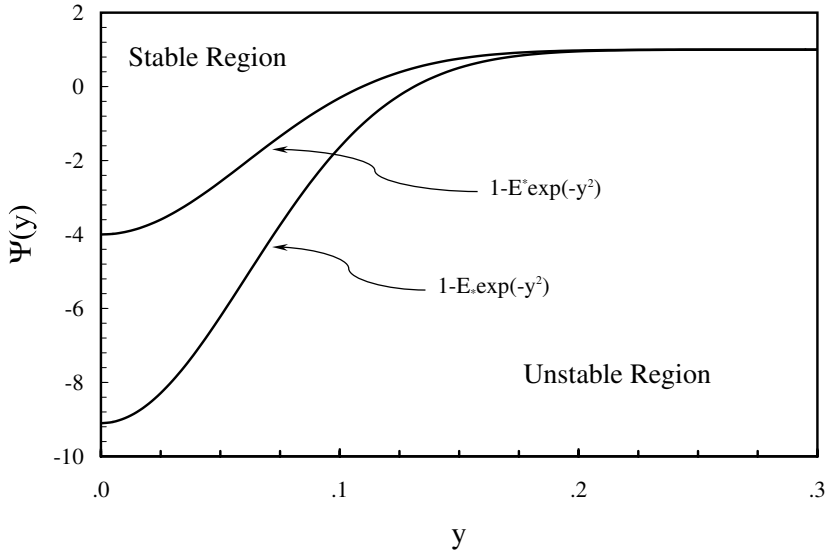

Figure 4. Regions of stability, $\Psi(y) \geqslant 1 - E^* \exp(-y^2)$, and instability, $\Psi(y) \leqslant 1 - E_* \exp(-y^2)$. A K value of unity was chosen for demonstration purposes.

This sufficient condition for stability can be complemented by the following sufficient condition for instability:

Condition 2 (Instability)**.** *Let $z \in \Omega_x$ be the solution of (7) for the equilibrium profile of the fluid interface subject to a local van der Waals stress. Furthermore, let $z(x)$ satisfy the constraint that $\Phi = \Phi(x, z(x))$ remains bounded as described above for all $x \in \mathbb{R}$. Then, there exists a positive constant E_* such that if*

$$\Phi(x) \leqslant \frac{1 - E\,\mathrm{e}^{-(x/l_G)^2}}{l_G^2} =: q(x) \qquad \forall x \in \mathbb{R} \tag{28}$$

for some $E > E_* > 5(3/2)^{3/2} \approx 9.186$, then the equilibrium profile will not be stable to arbitrary perturbations $v \in \Omega_x$. In fact, it is sufficient that

$$E > E_* = \tfrac{3}{32}\left[26\sqrt{6} + \sqrt{1944}\right] \approx 10.10$$

for instability.

As stated, the proofs of these two conditions follow from a direct application of lemmas 3 and 5, respectively, given in the appendix.

These conditions do *not* say that the function Φ need necessarily behave pointwise as a sum of a constant and a Gaussian (although the results shown in figure 3 are consistent with precisely this form), they only indicate limiting cases on which definitive stability statements can be founded. The results are illustrated in figure 4 which features, for $K = 1$, the two limiting boundary curves, $l_G^2 t(x) = K - E^* \exp(-x^2)$ and $l_G^2 q(x) = K - E_* \exp(-x^2)$, dividing the half plane into three regions. Equilibrium profiles giving rise to Φ-functions which lie *above* the upper solid curve, $t(x)$, fall into the category of profiles that are stable to all perturbations. Equilibrium profiles giving rise to Φ-functions which lie *below* the

lower solid curve, $q(x)$, fall into the category of profiles unstable to some perturbations (e.g., $w_1(x)$ used in the proof of lemma 5, in the appendix). Conditions 1 and 2 are, by their nature, sufficient conditions. Neither double as necessary conditions for stability or instability, respectively. Consequently, since $E^* \neq E_*$, there exists a third region in the half-plane about which nothing conclusive can be stated in either stability sense. Still, considerable insight into the stability–instability question can be obtained from conditions 1 and 2.

The comparisons made in figure 5 are self-explanatory. The results in both figures 5(a) and (b) suggest that the two uppermost Φ-curves correspond to equilibrium profiles that are stable to arbitrary small disturbances. Unfortunately, the stability properties of the remaining examples are not possible to establish. The interface profiles related to these lower plate heights clearly do not satisfy the assumptions of condition 2. Instead they either extend into or across the region bounded by the two stability limit curves where nothing definite can be said. Extension beyond this region, in the manner, say, of the lowest curve in figure 5(a) is quite suggestive of instability. However, with the tools presented here we cannot draw such a conclusion with any certainty. Given the exponential decay of the profile, it is singularly surprising that the Φ-function decays so much more rapidly. It is possible that its asymptotic approach to the limiting positive value may be exponential. However, this must take effect well after the observed initial, more rapid decay. In any case it is clearly not apparent on the scale of the figure.

Notwithstanding any incompatiabilities with present examples, one may still certainly conclude that condition 1 is an effective tool for indicating the possible stability of solutions to the Euler–Lagrange equation. The condition here takes obvious advantage of the fact that the calculated stability function, $\Phi(x)$, decays more rapidly than the Gaussian, $\sim\exp\left(-x^2/l_G^2\right)$, which characterizes the stability limit. Furthermore, given the rigorous argument which leads to condition 2, its value should not be underestimated; it too remains an unambiguous tool that is more appropriately used in circumstances where the stability function decays more slowly than the Gaussian. Unfortunately, its potential utility was not possible to demonstrate here.

5. Summary

This paper concerns an analysis of the stability of an infinite planar fluid–fluid interface subjected to a two-dimensional van der Waals stress arising from the presence of a solid two-dimensional plate positioned edge-on above the interface. The physical problem models, for example, the setup of a Wilhelmy plate experiment just prior to plate immersion through the air–water interface and three-phase contact line formation. However, the analysis and results are of wider validity. General results on the state of stability of a stressed fluid interface are established and expressed as conditions which are either sufficient to ensure a stable interface or an unstable interface. All the analyses focus on a sole, key function, $\Phi(x)$, of the equilibrium profile, $z(x)$, the latter a solution of the Euler–Lagrange equation for this problem. Our principal results are sufficient conditions for stability or instability based on a pointwise relation between $l_G^2\Phi(x)$ and the elementary function, $K - E\exp\left(-x^2/l_G^2\right)$. Through examples (figure 3) we have demonstrated the general functional behaviour of $\Phi(x)$ and its dependence on physical parameters. The examples give physical credence to the choice of stability limit functions, $K - E\exp\left(-x^2/l_G^2\right)$. The sufficient conditions proved in the appendix highlight special limiting values of the constant, E. Comparisons with actual cases (figure 5) indicate the potential applications of these sufficient conditions. In the given situations the stability condition is an effective limiting criterion as the stability function, Φ, decays much faster than the stability limit function, while the instability condition is less

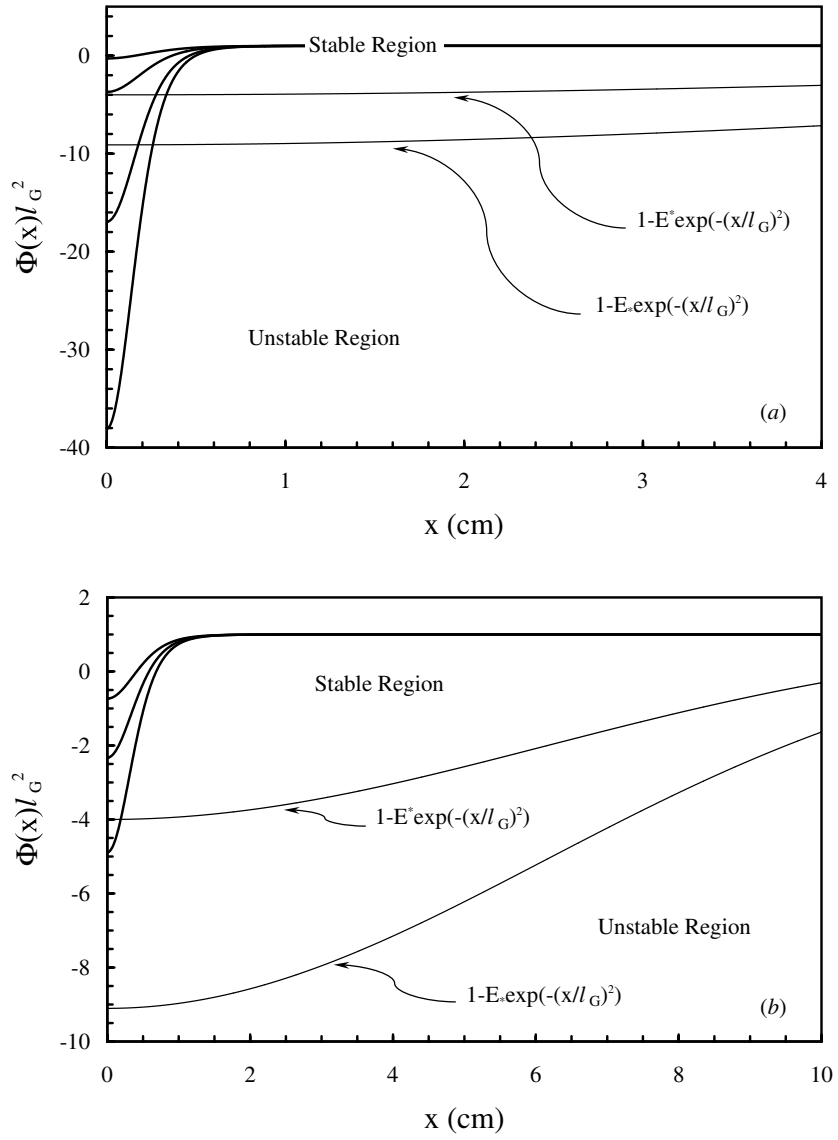

Figure 5. Comparison of the normalized stability function, Φl_G^2, with the stability limit functions defined in conditions 1 and 2. The thick solid lines correspond to computed stability functions for the van der Waals interaction between the fluid interface and a parabolic plate for a fixed splay parameter, $\lambda = 0.1$ m^{-1}. Other physical parameters are $\Delta\rho = 1$ kg m^{-3}, $\gamma = 72.8$ mN m^{-1}. In (*a*) $C_H = 10^{-21}$ J, and the curves (bottom to top) refer to plate heights of $z_{p0} = 2270, 2400, 3000, 4000$ nm. In (*b*) $C_H = 10^{-19}$ J and the curves (bottom to top) refer to plate heights of $z_{p0} = 9500, 10\,500, 12\,000$ nm. Thin solid lines are normalized stability limit functions, $t(x)l_G^2$ and $q(x)l_G^2$.

fruitful for the same reason, but would be more appropriate in cases involving slower decaying stability functions. Further efforts aimed at establishing sufficient as well as necessary stability or instability criteria that complement those given here are under way. Hopefully, it will be possible to develop criteria that are more appropriate to the observed behaviour.

Acknowledgments

This work was supported in part by a grant from the Carl Tryggers Foundation. The author thanks F P A Cortat for performing the calculations shown in figure 2 upon which the results shown in figures 3 and 5 are based.

Appendix

A.1. The Ritz analysis of stability–instability

In this appendix we review the essentials of the Ritz method [21] applied to the general functional

$$I[v] = \int_0^\infty \left[v_y^2 + \Psi(y)v^2\right] \mathrm{d}y. \tag{A1}$$

Independent and dependent variables, y and Ψ, are introduced in this and the next section to highlight the generality of the arguments presented. In this paper the properties of the Ritz method are exploited (in the next section) to provide a sufficient condition for instability.

The starting assumption is naturally that the functional, $I[v]$, does indeed possess a greatest lower bound. That is, there exists an $\overline{I}$ and a $\overline{v} \in \Omega_x$ such that

$$\overline{I} \leqslant I[\overline{v}] = \min_{v\in\Omega_x} I[v].$$

From Ω_x one constructs a set of N linearly independent members, denoted as $S = \{\phi_n\}_{n=1}^N$, and then generates a larger set, Φ_N, of functions of the form $\sum_{n=1}^N b_n\phi_n$, where the b_n are real constants. Obviously, Φ_N is a subspace of Ω_x. The point to the space, Φ_N, is that given an arbitrary $v \in \Omega_x$, an element ψ of the form $\sum_{n=1}^N b_n\phi_n$ can be found in Φ_N whose functional value, $I[\psi]$, approximates arbitrarily closely the functional value, $I[v]$. That is, for given $\epsilon > 0$, a ψ can be found in Φ_N such that $|I[v] - I[\psi]| < \epsilon$ for a given arbitrary $v \in \Omega_x$. Now, considering functions within Φ_N itself, there exists an element denoted by $u_N = \sum_{n=1}^N \overline{b}_n\phi_n$ that gives the least value to the multivariable function $G(b_1, b_{2,\ldots,}b_N) = I\left[\sum_{n=1}^N b_n\phi_n\right]$, so that $I[u_N] \leqslant I[\psi]$ for all $\psi \in \Phi_N$. If the integrand of I is a continuously differentiable function, then G will be a continuously differentiable function of $(b_1, b_2, \ldots, b_N)$ and u_N can be constructed from the solution of the set of N homogeneous equations

$$\frac{\partial G}{\partial b_n} = 0 \qquad n = 1, 2, \ldots, N. \tag{A2}$$

Clearly, the procedure has the property that $I[u_{N+1}] \leqslant I[u_N]$ since $\Phi_{N+1} \supset \Phi_N$ is a larger subset of Ω_x. Thus, the Ritz approach for given index $N < \infty$ provides an upper estimate of the minimum value of (A1).

Consider the subset of functions

$$S = \{y^{2n}\,\mathrm{e}^{-y^2}\}_{n\geqslant 0}$$

extracted from the set Ω_x. Let $\{b_n\}$ be a sequence of real numbers. The first member of S does not vanish at $x = 0$. In the present physical context an arbitrary perturbation constructed from members of S including the first member deforms the profile closer to or further away from the plate.

A.1.1. Optimization with respect to the set S. We consider fluctuations of the form

$$v(y) = \alpha\,\mathrm{e}^{-y^2} + \sum_{n=1}^N b_n y^{2n}\,\mathrm{e}^{-y^2} = \alpha\,\mathrm{e}^{-y^2} + \sum_{n=1}^N b_n\phi^{(n)} \tag{A3}$$

where b_n are constants to be optimized. As already remarked the perturbation gives a finite contribution at the origin, either bringing the profile up closer to the plate if $\alpha > 0$ or distancing it further if $\alpha < 0$. $|\alpha|$ thus determines the magnitude of the central displacement. The derivative of v

$$v_y = -2y\alpha\,\mathrm{e}^{-y^2} + \sum_{n=1}^{N} b_n 2y^{2n-1}\,\mathrm{e}^{-y^2}(n - y^2) = -2y\alpha\,\mathrm{e}^{-y^2} + \sum_{n=1}^{N} b_n \phi_y^{(n)}$$

so that

$$v^2 = \alpha^2\,\mathrm{e}^{-2y^2} + \sum_{n=1}^{N} b_n^2(\phi^{(n)})^2 + 2\alpha\,\mathrm{e}^{-y^2}\sum_{n=1}^{N} b_n\phi^{(n)} + 2\sum_{n=1}^{N-1}\sum_{m=n+1}^{N} b_n b_m \phi^{(n)}\phi^{(m)}$$

and

$$v_x^2 = 4x^2\alpha^2\,\mathrm{e}^{-2x^2} + \sum_{n=1}^{N} b_n^2\left(\phi_x^{(n)}\right)^2 - 4x\alpha\,\mathrm{e}^{-x^2}\sum_{n=1}^{N} b_n\phi_x^{(n)} + 2\sum_{n=1}^{N-1}\sum_{m=n+1}^{N} b_n b_m \phi_x^{(n)}\phi_x^{(m)}.$$

As before, we insert these results into the integral, $I[v]$, to form the function

$$G(b_1, b_2, \ldots, b_N) = I[\{b_n\}] = A + \sum_{n=1}^{N} b_n B_n + \sum_{m,m=1}^{N} b_n b_m C_{nm} \tag{A4}$$

where

$$\begin{cases} A = \alpha^2\int_0^\infty \left[4y^2\,\mathrm{e}^{-2y^2} + \Psi(y)\,\mathrm{e}^{-2y^2}\right]\mathrm{d}y \\ B_n = 2\alpha\int_0^\infty \left[\Psi(y)\,\mathrm{e}^{-y^2}\phi^{(n)} - 2y\,\mathrm{e}^{-y^2}\phi_y^{(n)}\right]\mathrm{d}y \qquad n = 1, 2, \ldots, N \\ C_{nm} = \int_0^\infty \left[\phi_y^{(n)}\phi_y^{(m)} + \Psi(y)\phi^{(n)}\phi^{(m)}\right]\mathrm{d}y \qquad n, m = 1, 2, \ldots, N. \end{cases} \tag{A5}$$

Differentiating in turn with respect to the variable coefficients $(b_1, b_2, \ldots b_N)$ and setting the derivatives to zero, in accordance with (A2), leads to N equations in the N unknowns $\{\overline{b}_n\}$

$$\sum_{m=1}^{N} C_{nm}\overline{b}_m + B_n = 0 \qquad n = 1, 2, \ldots, N. \tag{A6}$$

The first approximation ($N = 1$) in this case reads

$$\overline{b}_1 = -\frac{B_1}{C_{11}} = -\alpha\frac{\int_0^\infty [\Psi(y) - 4(1 - y^2)]y^2\,\mathrm{e}^{-2y^2}\,\mathrm{d}y}{\int_0^\infty [4(1 - y^2)^2 + \Psi(y)y^2]y^2\,\mathrm{e}^{-2y^2}\,\mathrm{d}y} \tag{A7}$$

and the approximation to the minimum value, $I[u_1 = \alpha\,\mathrm{e}^{-y^2} + \overline{b}_1\phi^{(1)}]$, is given by

$$\begin{aligned} \min_{v\in\Omega_x} I[v] \leqslant I[u_1] &= A - \frac{B_1^2}{C_{11}} \\ &= \alpha^2\int_0^\infty [4y^2 + \Psi(y)]\,\mathrm{e}^{-2y^2}\,\mathrm{d}y - \alpha^2\frac{\left[\int_0^\infty [\Psi(y) - 4(1 - y^2)]y^2\,\mathrm{e}^{-2y^2}\,\mathrm{d}y\right]^2}{\int_0^\infty [4(1 - y^2)^2 + \Psi(y)y^2]y^2\,\mathrm{e}^{-2y^2}\,\mathrm{d}y}. \end{aligned} \tag{A8}$$

In the application of the Ritz method we can drop the unimportant factor of α^2 since only the sign of (A8) is important.

A.2. Inequalities concerning the functional $I[v] = \int_0^\infty \left[v_y^2 + \Psi(y)v^2\right] \mathrm{d}y$

In this appendix we consider the functional

$$I[v] = \int_0^\infty \left[v_y^2 + \Psi(y)v^2\right] \mathrm{d}y$$

and establish sufficient conditions on the function Ψ which ensure that $I[v]$ is either strictly positive or strictly negative for all $v \in \Omega_x$. We suppose that $\Psi \in L_2(\mathbb{R})$, that it is an even function and that there exist numbers $K, E > 0$ such that

$$\begin{cases} K - E < \Psi < K & \text{for all} \quad y \in \mathbb{R} \\ \Psi \to K & \text{as} \quad |y| \to \infty. \end{cases} \tag{A9}$$

We then have the following lemmas on positivity and negativity of $I[v]$:

Lemma 3 (Positivity)**.** *Let* $\Psi = \Psi(y)$ *satisfy the above conditions on continuity, integrability and boundedness for all* $y \in \mathbb{R}$*. Let* $K > 0$ *be given. Then, there exists a positive constant* E^* *such that if*

$$\Psi(y) \geqslant K - E\,\mathrm{e}^{-y^2} =: t(y) \qquad \forall y \in \mathbb{R} \tag{A10}$$

for some $E \leqslant E^*$ *then the functional* $I[v]$ *will be strictly positive for arbitrary* $v \in \Omega_x$*. In fact,* $E^* = 4 + K$*.*

A proof relies on the use of the following lemma which is of interest in its own right. Firstly, define $L_w^2(\mathbb{R})$ to be the space of continuous functions which are square integrable over the real line with respect to the weight function $w(y) := \exp(-y^2)$. That is

$$L_w^2(\mathbb{R}) = \left\{ u \in C(\mathbb{R}); \int_{-\infty}^{\infty} \mathrm{e}^{-y^2} |u|^2 \,\mathrm{d}y < \infty \right\}.$$

It is known [24] that $L_w^2(\mathbb{R})$ is a Hilbert space equipped with the inner product

$$(u, v)_w := \int_{-\infty}^{\infty} w(y)u(y)v(y)\,\mathrm{d}y = \int_{-\infty}^{\infty} \mathrm{e}^{-y^2} u(y)v(y)\,\mathrm{d}y$$

and that the set $\{H_n(y)\}_{n=0}^{\infty}$ of Hermite polynomials

$$H_k(y) = (-1)^k\,\mathrm{e}^{y^2} \frac{\mathrm{d}^k}{\mathrm{d}y^k}\,\mathrm{e}^{-y^2}$$

forms a dense, complete subset of $L_w^2(\mathbb{R})$. Consequently, any $u \in L_w^2(\mathbb{R})$ can be expressed as a series of the form

$$u = \sum_{n=0}^{\infty} a_n H_n(y) \qquad y \in \mathbb{R}$$

the convergence being uniform. We now state the lemma.

Lemma 4. *Let* $u_y, u \in L_w^2(\mathbb{R})$*. Then,*

$$\int_{-\infty}^{\infty} \mathrm{e}^{-y^2} u_y^2 \,\mathrm{d}y > 2 \int_{-\infty}^{\infty} \mathrm{e}^{-y^2} u^2 \,\mathrm{d}y \tag{A11}$$

unless u *is a constant function.*

This result is likely to be well known. However, we have not found it in any of the standard texts [25].

Proof. As stated above, any function $u \in L^2_w(\mathbb{R})$ can be represented in a series of the form

$$u = \sum_{n=0}^{\infty} a_n H_n(y) \qquad y \in \mathbb{R}.$$

By assumption the convergence is uniform and since $u_y \in C(\mathbb{R})$, its expansion is equal, in the distributional sense, to the pointwise derivative of the above series representation. Assuming uniform convergence of the various series, the processes of summation and integration can be interchanged and we therefore have

$$\begin{aligned}\int_{-\infty}^{\infty} \mathrm{e}^{-y^2} u_y^2 \,\mathrm{d}y &:= \int_{-\infty}^{\infty} \mathrm{e}^{-y^2} \left[\sum_{n=1}^{\infty} a_n \frac{\mathrm{d}}{\mathrm{d}y} H_n(y)\right]^2 \mathrm{d}y \\ &= \int_{-\infty}^{\infty} \mathrm{e}^{-y^2} \left[\sum_{n=1}^{\infty} a_n^2 \left[\frac{\mathrm{d}}{\mathrm{d}y} H_n(y)\right]^2 + 2\sum_{n=1}^{\infty}\sum_{m=n+1}^{\infty} a_n a_m \frac{\mathrm{d}H_n}{\mathrm{d}y}(y)\frac{\mathrm{d}H_m}{\mathrm{d}y}(y)\right] \mathrm{d}y \\ &= \int_{-\infty}^{\infty} \mathrm{e}^{-y^2} \left[\sum_{n=1}^{\infty} a_n^2 [2n H_{n-1}(y)]^2 + 2\sum_{n=1}^{\infty}\sum_{m=n+1}^{\infty} a_n a_m 4nm H_{n-1}(y) H_{m-1}(y)\right] \mathrm{d}y\end{aligned}$$

where we have used the identity

$$\frac{\mathrm{d}}{\mathrm{d}y} H_k(y) = 2k H_{k-1}(y)$$

to obtain the last equality. Furthermore, using the orthogonality property of the polynomials

$$\int_{-\infty}^{\infty} \mathrm{e}^{-y^2} H_k(y) H_l(y) \,\mathrm{d}y = 2^k k! \sqrt{\pi} \delta_{kl}$$

with respect to the given inner product we obtain

$$\begin{aligned}\int_{-\infty}^{\infty} \mathrm{e}^{-y^2} u_y^2 \,\mathrm{d}y &= \sum_{n=1}^{\infty} a_n^2 [2n]^2 2^{n-1} (n-1)! \sqrt{\pi} \\ &= 2\sum_{n=1}^{\infty} a_n^2 n 2^n n! \sqrt{\pi} = 2\sum_{n=0}^{\infty} a_n^2 n 2^n n! \sqrt{\pi} \\ &> 2\sum_{n=0}^{\infty} a_n^2 2^n n! \sqrt{\pi} =: 2\int_{-\infty}^{\infty} \mathrm{e}^{-y^2} u^2 \,\mathrm{d}y.\end{aligned}$$

The last result being an identity for a uniformly convergent series of Hermite functions. This inequality is valid unless $a_n = 0$ for $n > 0$ in which case the sign of the inequality is reversed if in addition $a_0 \neq 0$, or replaced by equality if $a_0 = 0$. That is, the inequality holds unless u is constant. The lemma is proved. □

Proof of lemma 3. Under the stated assumption we have

$$I[v] = \int_0^{\infty} \left(v_y^2 + \Psi(y) v^2\right) \mathrm{d}y > \int_0^{\infty} \left(v_y^2 + \left(K - E\,\mathrm{e}^{-y^2}\right) v^2\right) \mathrm{d}y = I^t[v]. \tag{A12}$$

Positivity is clearly guaranteed in the event that $E < K$, we are therefore interested in positive values of $E > K$. For any given $v \in \Omega_x$, the last integral defines a function $g(E; v)$

$$g(E; v) = \int_0^{\infty} \left(v_y^2 + \left(K - E\,\mathrm{e}^{-y^2}\right) v^2\right) \mathrm{d}y$$

with the properties

$$\begin{cases} g(K, v) > 0 \\ g_E(E; v) = -\int_0^\infty \mathrm{e}^{-y^2} v^2 \, \mathrm{d}y < 0 \end{cases}$$

for any $v \in \Omega_x$. Consequently, g decreases monotonically with E from some positive value at $E = K$. Therefore, there exists a maximum value of E, $E^* > K$, for which the integral remains positive for all $v \in \Omega_x$.

We now utilize the inequality provided in the above lemma, or rather a modified version of it, to establish the value of E^*. Clearly, the inclusion $\Omega_x \subset L^2_w(\mathbb{R})$ is true. Since elements in Ω_x are even functions of the independent variable we must have that any $v \in \Omega_x$ can be expressed in the form

$$v = \sum_{n=0}^{\infty} a_n H_{2n}(y) \qquad y \in \mathbb{R}$$

where $H_{2n}(x)$ are the even Hermite functions of x. Invoking this special case in the proof of the lemma shows that for functions in Ω_x, inequality (A11) can be replaced by

$$\int_{-\infty}^{\infty} \mathrm{e}^{-y^2} v_y^2 \, \mathrm{d}y \geqslant 4 \int_{-\infty}^{\infty} \mathrm{e}^{-y^2} v^2 \, \mathrm{d}y.$$

Note also that since nonzero constant functions cannot belong to Ω_x it is unnecessary to explicitly stipulate the additional restriction given in the lemma. The equality in this last result covers the case of the zero function. Implementing this inequality gives

$$\begin{aligned} I^t[v] &= \int_0^\infty \left(v_y^2 + \left(K - E\,\mathrm{e}^{-y^2}\right)v^2\right) \mathrm{d}y > \int_0^\infty v_y^2 + (K - E)\,\mathrm{e}^{-y^2} v^2 \, \mathrm{d}y \\ &= \int_0^\infty v_y^2 \, \mathrm{d}y - (E - K) \int_0^\infty \mathrm{e}^{-y^2} v^2 \, \mathrm{d}y \\ &\geqslant \int_0^\infty v_y^2 \, \mathrm{d}y - \frac{(E - K)}{4} \int_0^\infty \mathrm{e}^{-y^2} v_y^2 \, \mathrm{d}y \\ &= \int_0^\infty \left[1 - \frac{(E - K)}{4}\,\mathrm{e}^{-y^2}\right] v_y^2 \, \mathrm{d}y. \end{aligned}$$

Without question, if $E \leqslant 4 + K$, then

$$I[v] \geqslant I^t[v] \geqslant \int_0^\infty \left[1 - \frac{(E - K)}{4}\mathrm{e}^{-y^2}\right] v_y^2 \, \mathrm{d}y > 0 \qquad \text{for all} \quad v \in \Omega_x.$$

This last inequality establishes the sought after value of $E^* = 4 + K$. □

This sufficient condition for positivity can be complemented by the following sufficient condition for negativity.

Lemma 5 (Negativity). *Let $\Psi = \Psi(y)$ satisfy the above conditions on continuity, integrability and boundedness for all $y \in \mathbb{R}$. Let $K > 0$ be given. Then, there exists a positive constant E_* such that if*

$$\Psi(y) \leqslant K - E\,\mathrm{e}^{-y^2} =: q(y) \qquad \forall y \in \mathbb{R} \tag{A13}$$

for some $E > E_* > (7 + 3K)(3/2)^{3/2}/2$, then the functional $I[v]$ can take negative values for some $v \in \Omega_x$. In fact, it is sufficient that

$$E > E_* = 3\left[(29 - 3K)\sqrt{6} + \sqrt{3894 - 4500K + 2550K^2}\right]/32$$

for negativity to arise.

Proof. The proof follows from the Ritz analysis above, assisted by the following integrals:

$$\begin{cases} C_* = \int_0^\infty \left[4(1-y^2)^2 - \left(K - E\,\mathrm{e}^{-y^2}\right)y^2\right]y^2\,\mathrm{e}^{-2y^2}\,\mathrm{d}y = (7+3K)\frac{\sqrt{2\pi}}{64} - \frac{E}{72}\sqrt{3\pi} \\ A_* = \int_0^\infty \left[4y^2 - \left(K - E\,\mathrm{e}^{-y^2}\right)\right]\mathrm{e}^{-2y^2}\,\mathrm{d}y = (1+K)\frac{\sqrt{2\pi}}{4} - \frac{E\sqrt{3\pi}}{6} \\ B_* = -\int_0^\infty \left[D\,\mathrm{e}^{-y^2} + 4(1-y^2)\right]y^2\,\mathrm{e}^{-2y^2}\,\mathrm{d}y = \left(K - \frac{1}{4}\right)\frac{\sqrt{2\pi}}{4} - \frac{E}{36}\sqrt{3\pi}. \end{cases} \tag{A14}$$

An important feature of the Ritz theory is that the sequence of approximate minimizers, $\{u_m\}$, with u_m defined as in (A3) but using the optimally determined coefficients, $\{\overline{b}_n\}$, of section 4.1, leads to the following sequence of inequalities

$$\min_{v\in\Omega_x} I[v] \leqslant \cdots \leqslant I[u_{N+1}] \leqslant I[u_N] \leqslant \cdots \leqslant I[u_2] \leqslant I[u_1]. \tag{A15}$$

However, if $\Psi(y) \leqslant K - E\,\mathrm{e}^{-y^2}$ for all $y \in \mathbb{R}$ then clearly

$$I[v] \leqslant I^q[v] := \int_0^\infty \left[v_y^2 + \left(K - E\,\mathrm{e}^{-y^2}\right)v^2\right]\mathrm{d}y \qquad \forall v \in \Omega_x. \tag{A16}$$

In particular, inequality (A16) holds for any member of the Ritz set of minimizers $\{u_m\}$. Consequently, negativity would be guaranteed if one can show that any $I^q[u_m]$ in the sequence

$$\cdots \leqslant I^q[u_{N+1}] \leqslant I^q[u_N] \leqslant \cdots \leqslant I^q[u_2] \leqslant I^q[u_1].$$

is negative.

Denote by $\{w_m\}$ the sequence of Ritz minimizers of $I^q[v]$ defined in (A16) having the form (A3) with optimized coefficients $\{\overline{b}_n\}$ determined as outlined in section 4. Using the integrals defined in (A5) we have for $N = 1$ that

$$\min_{v\in\Omega_x} I[v] \leqslant I[u_1] = A - \frac{1}{C_{11}}B_1^2 \leqslant I^q[u_1] = \int_0^\infty \left[(u_1)_y^2 + \left(K - E\,\mathrm{e}^{-y^2}\right)u_1^2\right]\mathrm{d}y$$

according to (A16). Moreover, we find that

$$\begin{aligned} A - \frac{1}{C_{11}}B_1^2 &\leqslant A_* - \frac{1}{C_*}B_1^2 \\ &\leqslant A_* + \frac{1}{|C_*|}B_1^2 \\ &\leqslant A_* + \frac{1}{|C_*|}(B_*)^2 =: I^q[w_1]. \end{aligned}$$

The first inequality is valid provided $C_{11} < C_* < 0$ and this will be true if $E > (7+3K)(3/2)^{3/2}/2 \approx 6.43$ for $K = 0$. By inspection, (A14) leads to the asymptotic behaviour

$$I^q[w_1] \longrightarrow (1+K)\frac{\sqrt{2\pi}}{4} - \frac{\sqrt{3\pi}}{9}E$$

as $E \to \infty$. Consequently, for E large enough, $I^q[w_1]$ will be negative, by the preceding inequality. To complete the proof we need only to find the smallest value of E for which $I^q[w_1]$, on the branch converging to this asymptotic, will be negative. Since $I^q[w_1]$ is quadratic in E, the largest of the two roots of $I^q[w_1]$ will naturally be the one of interest. This root is quoted in the theorem. Its approximate value for $K = 0$ is $E^* \simeq 12.5097$, while it achieves an absolute minimum value of $(E_*)_{\min} = \min_K E_* = 33\sqrt{6}/8 \simeq 10.10$ when $K \simeq 1.01$. Thus, for any $E > E_*$, the functional can take negative values for some functions. Note that it is easy to confirm by elementary means that the condition $E_* = E_*(K) \geqslant (7+3K)(3/2)^{3/2}/2$ ensuring $C_* = -|C_*| < 0$ is satisfied for all K values. Equality occurs at a single point of tangency, at the value $K \simeq 1.8$. □

Note that if in the proof of the preceding lemma we considered a Ritz approximation of higher order than the first ($N = 1$), then the above generous estimate of E_* would be reduced, bringing the lower curve in figure 4 up toward $t(y)$.

References

[1] Gaines G L 1966 *Insoluble Monolayers at Liquid–Gas Interfaces* (New York: Wiley)
[2] MacRitchie F 1990 *Chemistry at Interfaces* (New York: Academic)
[3] Mozaffary H 1991 *Chem. Phys. Lipids* **59** 39
[4] Birdi K S 1973 *J. Colloid Interface Sci.* **43** 545
[5] Lundh G, Eliasson A-C and Larsson 1988 *J. Cereal Sci.* **7** 1
[6] Miklavic S J and Thulin E 1995 *J. Colloid Interface Sci.* **171** 256
[7] Miklavic S J 1995 *J. Colloid Interface Sci.* **171** 446
[8] Israelachvili J N 1992 *Intermolecular and Surface Forces* 2nd edn (New York: Academic)
[9] Ruckenstein E and Jain R K 1974 *J. Chem. Soc. Faraday II* **70** 132
[10] Jain R K and Ruckenstein E 1976 *J. Colloid Interface Sci.* **54** 108
[11] Oron A, Davis S H and Bankoff S G 1997 *Rev. Mod. Phys.* **69** 931
[12] Zhang W W and Lister 1999 *Phys. Rev. Lett.* **83** 1151
Zhang W W and Lister 1999 *Phys. Fluids* **11** 2454
[13] Churaev N V, Starov V M and Derjaguin B V 1982 *J. Colloid Interface Sci.* **89** 16
[14] Forcada M L 1993 *J. Chem. Phys.* **98** 638
[15] Forcada M L, Arista N R, Gras-Marti A, Urbassek H M and Garcia-Molina R 1991 *Phys. Rev.* B **44** 8226
[16] Cortat F P A and Miklavcic S J 2003 *Phys. Rev. Lett.* submitted
[17] Cortat F P A and Miklavcic S J 2003 *Phys. Rev.* E submitted
[18] Miklavcic S J 2001 *ITN Research Report Series* (LiTH-ITN-R-2001-11, ISSN 1650-2612)
[19] Courant R and Hilbert D 1965 *Methods of Mathematical Physics* vol 1 (New York: Wiley) ch 4
[20] Ewing G M 1985 *Calculus of Variations with Applications* (New York: Dover. Original publication Norton & Co, 1969)
[21] Morse P M and Feschbach H 1952 *Methods of Theoretical Physics* vol 2 (New York: McGraw-Hill)
[22] Miklavcic S J and Attard P 2001 *J. Phys. A. Math. Gen.* **34** 7849
[23] Miklavcic S J and Attard P 2002 *J. Phys. A. Math. Gen.* **35** 4335
[24] Renardy M and Rogers R C 1992 *An Introduction to Partial Differential Equations* (New York: Springer)
[25] Hardy G H, Littlewood J E and Polya G 1952 *Inequalities* 2nd edn (Cambridge: Cambridge University Press)